Design and Fabrication of a Lowpass Filter using a New Butterfly-Shaped Defected Ground Structure

Majeed Rashid Zaidan[1], Vahid Rezaeian[2], Saber Izadpanah Toos[3*]
1- Middle Technical University, Electrical Technical Department, Baghdad, Iraq.
Email: majeedrzn@mtu.edu.iq
2- Ferdowsi University, Department of Electrical Engineering, Mashhad, Iran.
Email: vrezaiyan@yahoo.com
3- Sadjad University of Technology, Department of Electrical Engineering, Mashhad, Iran.
Email: s.izadpanah220@sadjad.ac.ir (Corresponding author)

Received: April 2021 Revised: June 2021 Accepted: August 2021

ABSTRACT:
In this paper, a new Defected Ground Structure (DGS) is introduced and analyzed. The effect of the structure's dimensions on the location of the attenuation pole and the cutoff frequency to study the frequency characteristics is investigated. In the following, a lowpass filter with 3 dB cutoff frequency at 3 GHz is designed and optimized using the proposed defected ground structure, and its frequency characteristic is reported. The designed lowpass filter is fabricated to verify the simulation process. Also, simulation results, the equivalent circuit, and the measured results with the Network Analyzer are compared.

KEYWORDS: Defected Ground Structure, DGS, Low-pass Filter, Microstrip Filter.

1. INTRODUCTION

In recent decades, defected ground structures have been the focus of many researchers. These structures are used in many devices, such as antennas, filters, couplers, and power dividers [1-11]. In general, the defected ground structure consists of a periodic or non-periodic defect on the ground plane of the flat transmission lines created by modification and development of the bandgap structures (PBG, EBG) [12]. The defect on the ground plane will cause a change in the current on the ground plane, resulting in changes in transmission line characteristics, including capacitance and inductance of a line. In general, it can be said that any defect on the ground plane increases the inductance and the effective capacitance of the transmission line. In the bandgap structures, many parameters such as number, geometrical shape, and formation of the networks affect the bandgap of the structure. Therefore, the modeling of bandgap structures is complicated. Unlike bandgap structures, defected ground structures can be modeled using simple equivalent circuits composed of compact elements. Also, due to many periodic defects in bandgap structures, it is more challenging to analyze such structures than defected ground structures.

In Fig. 1, the microstrip transmission line is shown with a rectangular defect on the ground plane. This type of structure is known as the dumbbell-shaped DGS and is the first defected structure introduced [13]. The defected ground structures consist of a microstrip line on a substrate and one or more defects created on the ground.

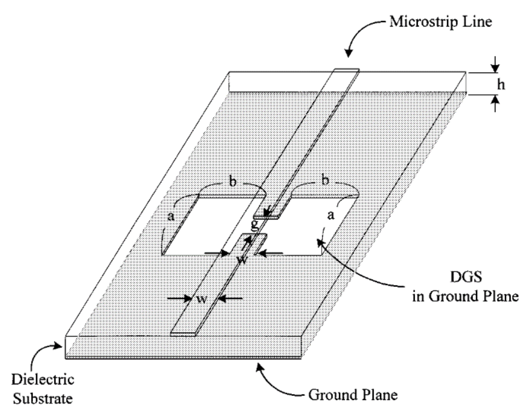

Fig. 1. Schematic of DGS [13].

Defected ground structures have different shapes. These include square, circular, triangular, and more complex shapes [14-17]. The narrow and wide areas on

Paper type: Research paper
DOI: https://doi.org/10.52547/mjtd.10.3.129
How to cite this paper: M. R. Zaidan, V. Rezaeian and S. Izadpanah Toos, "**Design and Fabrication of a Lowpass Filter using a New Butterfly-Shaped Defected Ground Structure**", Majlesi Journal of Telecommunication Devices, Vol. 10, No. 3, pp. 129-136, 2021.

the ground plane increase the effective capacitance and inductance of the line. The creation defect on the ground plane changes the distribution of available surface currents on the ground plane; this affects the values of effective capacitance and inductance of the line. The frequency characteristic of the scattering parameters of a sample of dumbbell-shaped DGS is shown in Fig. 2.

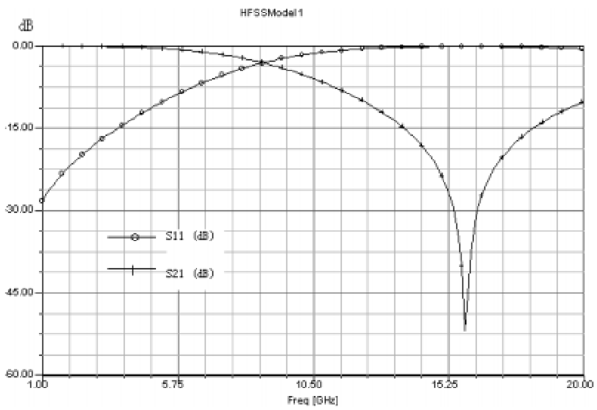

Fig. 2. The frequency characteristic of DGS [13].

A defected ground structure has features such as cutoff band, slow-wave effect, and high impedance. In general, DGS has the following advantages compared with the bandgap structure:

- Have smaller geometric dimensions. In other words, by using several defect elements on the ground plane, characteristics similar to the periodic bandgap structures can be achieved.
- The frequency characteristic of the scattering parameters of the dumbbell-shaped DGS can be matched by the frequency response of a unipolar Butterworth filter.
- A defected ground structure cell has relatively small geometrical dimensions, and by putting a few of them alternately together, the slow-wave effect can be realized.
- It is easier to analyze, design, and employ defected ground structures to realize passive microwave devices compared with bandgap structures.

In this paper, a novel DGS is proposed, and the frequency characteristics of this structure are investigated. The organization of this paper is as follows. In section 2, the equivalent circuit for the defected ground structure is presented. In section 3, butterfly-shaped DGS is introduced. The effect of changing the dimensions on the frequency characteristic is investigated in section 4. In section 5, a lowpass filter using a butterfly-shaped DGS is designed. Comparison of the designed filter using the butterfly-shaped DGS and designed filter using complementary split-ring resonator (CSRR) defected ground structure are presented in section 6. In section 7, simulation and measurement results of the designed filter using butterfly-shaped DGS are compared, and finally, the conclusion is given.

2. THE EQUIVALENT CIRCUIT FOR THE DEFECTED GROUND STRUCTURES

As can be seen in Fig. 2, a cell of these structures produces an attenuation pole at a specified frequency. Since the frequency characteristics of the defected ground structures are similar to the parallel LC resonant circuit, they can be simulated with a parallel LC equivalent circuit. For example, the rectangular sections and their connecting arm are equated to the inductor and capacitor in a dumbbell-shaped structure, respectively. By resizing these two parts, the inductor and capacitor values of the equivalent circuit also change. The equivalent circuit for the defected ground structure and the lowpass unipolar Butterworth filter is shown in Fig. 3.

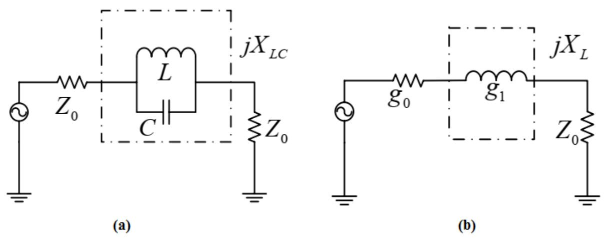

Fig. 3. The equivalent circuit of (a) the microstrip line with the defected ground structure, (b) the lowpass unipolar Butterworth filter [18].

The values of inductance and capacitance of the LC equivalent circuit of defected ground structures derive from the relationships existing for the equivalent circuit of the DGS and the unipolar Butterworth filter. How to determine the equivalent circuit elements of a structure is given in (1) to (3) [18].

$$X_{LC} = \frac{\omega}{C} \frac{1}{(\omega_0{}^2 - \omega^2)} \tag{1}$$

$$X_L = \Omega Z_0 g_1 \tag{2}$$

$$X_{LC}|_{\omega=\omega_{c,3dB}} = X_L|_{\Omega=1} \tag{3}$$

In these equations, Ω is the normalized angular frequency, $g_1 = 2$ is the normalized value of the unipolar Butterworth sample filter element, $Z_0 = 50\Omega$ is the characteristic impedance of the line, and ω_0 is the resonant frequency [15].

3. INTRODUCING THE BUTTERFLY-SHAPED DEFECTED GROUND STRUCTURE

Fig. 4 shows a general view of the butterfly-shaped DGS. The structure consists of a 50 Ω microstrip line above the substrate and a butterfly-shaped dumbbell cell removed from the ground plane. This structure has four variable parameters *a*, *b*, *c*, and *g*; changing these parameters can change the location of the attenuation pole and the cutoff frequency. The capacitance of the structure can be changed by changing the parameter *c* from zero to *a/2* and assuming the connecting arm as a capacitor. This feature enables the designer to increase the capacitor plates length by increasing *c*, thereby achieving higher capacitance with *a* specified *g*. Therefore, parameter *c* can be considered as one of the essential advantages of the butterfly-shaped DGS over the square dumbbell-shaped DGS. Other benefits of this structure over the square dumbbell-shaped DGS are reducing the area of the structure for a given resonant frequency and increasing the *Q* of the structure.

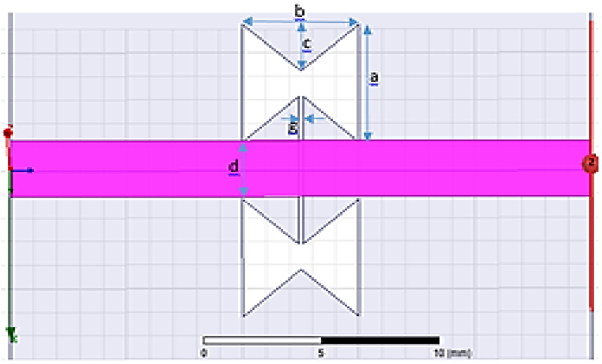

Fig. 4. Top view of a butterfly-shaped DGS.

The frequency characteristic of the butterfly-shaped DGS with dimensions *a=b=2.67mm*, *c=1mm*, and *g=0.2mm* is shown in Fig. 5. The substrate used in this structure is RT/Duroid 5880 with dielectric constant (relative permittivity) *εr=2.2* and thickness *d=0.7874mm*. HFSS software is used for simulation, full-wave analysis, and optimization of structure parameters. According to the frequency characteristic shown in Fig. 5, this structure has an attenuation pole at 9.02GHz and a 3 dB cutoff frequency at 6.45GHz. Also, in Fig. 5, the frequency characteristic of a square dumbbell-shaped DGS with an attenuation pole of 9.02GHz is plotted. Therefore, dimensions of this structure to achieve a frequency characteristic similar to the butterfly-shaped DGS are *a=b=3.02mm* and *g=0.2mm*.

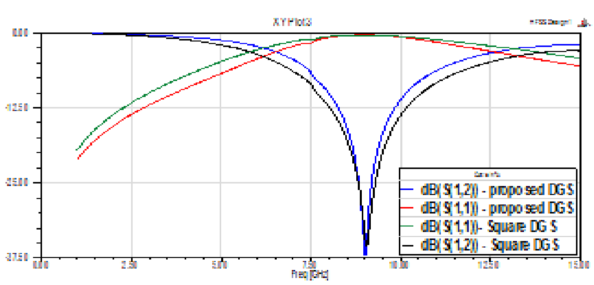

Fig. 5. The frequency characteristic of butterfly-shaped DGS and square dumbbell-shaped DGS.

As can be seen in Fig. 5, the filter bandwidth of the butterfly-shaped DGS is 12.94% higher than the square dumbbell-shaped DGS at the same resonant frequency. Also, in terms of dimensions, the butterfly-shaped DGS has a 21.82% decrease in surface area than the square dumbbell-shaped DGS.

4. INVESTIGATING THE EFFECT OF CHANGING THE DIMENSIONS ON THE FREQUENCY CHARACTERISTIC

The following three conditions are considered to investigate the effect of the dimensions of the proposed DGS on its frequency characteristic:

4.1. *a, b, c*=constant, *g*=variable.

In this case, *a=b=5mm* and *c=2mm* are assumed, and *g* is changed in the 0.1mm to 1mm range with 0.1mm intervals. The plots in Fig. 6 show the effect of changing the parameter *g* on the frequency characteristic of the proposed DGS.

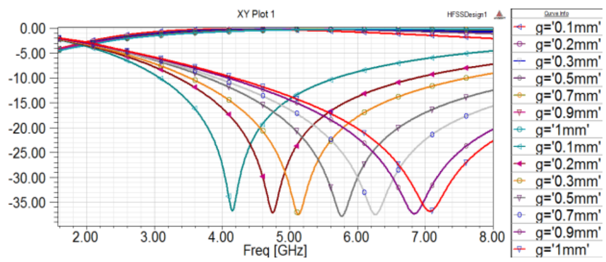

Fig. 6. Frequency characteristic (a = b = 5mm, c = 2mm and g from 0.1mm to 1mm).

As shown in Fig. 6, the cutoff frequency increases with increasing *g*, and the location of the attenuation pole is shifted to higher frequencies. This behavior can be explained by the fact that with increasing g, the equivalent capacitance decreases, which causes an increase in the resonant frequency.

4.2. *g, c*=constant, *a, b*=variable.

In this case, *g=0.2mm* and *c=1mm* are considered, and the parameters *a* and *b* are equal and vary from 3.5mm to 6mm with 0.5mm intervals.

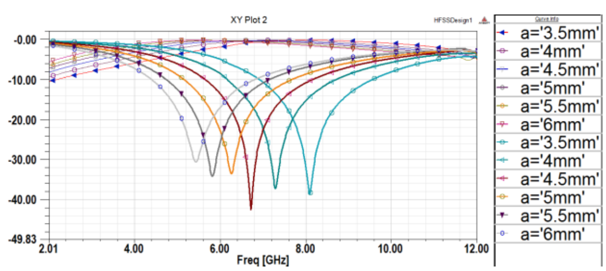

Fig. 7. Frequency characteristic (a = b = 3.5 to 6mm, c = 1mm and g= 0.2mm).

As shown in Fig. 7, as the area of the structure increases (increasing the size of a and b), the cutoff frequency decreases, and the attenuation pole shifts to lower frequencies. The change of the attenuation pole location toward lower frequencies can be justified by increasing the area of the structure. An increasing area of the structure causes the flow of return currents at the ground plane around the proposed DGS to increase. Therefore, the effective inductance of the transmission line is increased. Finally, an increase in the equivalent Inductance of the structure reduces the cutoff frequency and shifts the attenuation pole to lower frequencies.

4.3. *a, b, g*=constant, *c*=variable.

In this case, $a=b=5mm$ and $g=0.2mm$ are assumed, and c is changed from 0.5mm to 2mm. As shown in Fig. 8, as the parameter c increases, the location of the attenuation pole shifts to lower frequencies. However, unlike the previous two cases, the cutoff frequency is approximately constant.

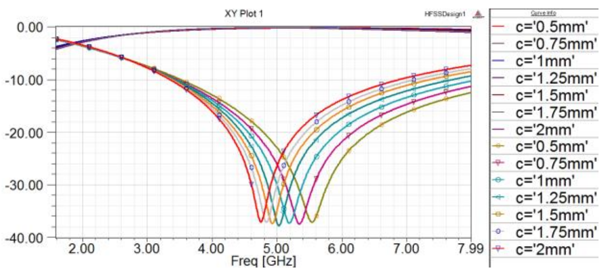

Fig. 8. Frequency characteristic (a = b = 5mm, g= 0.2mm and c= 0.5 to 2mm).

5. DESIGN OF A LOWPASS FILTER USING A BUTTERFLY-SHAPED DGS

Microwave filters are the elements that provide frequency selection in satellite communications, mobile communications, radar, and electronic warfare systems at microwave frequencies. Many applications require a lowpass filter to remove unwanted harmonics and signals, such as mixers and oscillators. Broad stopband bandwidth to eliminate these signals, linear passband, and small dimensions are among the essential parameters in the design of these filters. Although conventional methods of designing lowpass filters have a simple design, the disadvantage of these structures is the lack of broad stopband bandwidth. Recently, various methods have been introduced for the manufacture of filters with broad stopband bandwidth, one of which is the use of defected ground structures.

In this section, a five-pole Chebyshev filter with a 0.01dB ripple and 3 dB cutoff frequency at 3 GHz is designed using the proposed defected ground structure. The substrate used in this design is the CER-10 (Taconic) with a relative permittivity $\varepsilon r = 10$ and a thickness $d = 0.625mm$. One way to design lowpass filters in the microwave frequency range is to replace the inductive elements of the lowpass sample filter with defected ground structures. In this method, the inductors in the compressed circuit of the sample filter are replaced with a parallel LC circuit. Then, the final filter is obtained by placing a DGS with appropriate dimensions instead of each of the LC circuits. Fig. 9 shows the compressed circuit of a five-pole Chebyshev filter. In this circuit, *gi* (i=1, 2, 3, 4, and 5) are the normalized values of the filter elements. The values of *gi* are obtained according to the graphs and tables in [19].

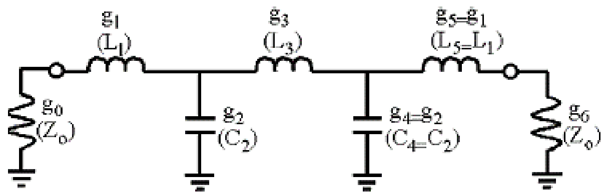

Fig. 9. The compressed circuit of a five-pole Chebyshev filter [19].

Then, according to the characteristic impedance of the line ($Z_0 = 50\Omega$) and the cutoff frequency (3 GHz) in the desired filter, the values of the circuit elements are determined by performing impedance and frequency transformations by the equations 4 to 6 [19].

$$C_2 = \left(\frac{R_0'}{R_0}\right)\left(\frac{w_1'}{w_1}\right) g_2 = \frac{g_2}{Z_0 w_c} = \frac{g_4}{Z_0 w_c} = C_4 \tag{4}$$

$$L_1 = \left(\frac{R_0}{R_0'}\right)\left(\frac{w_1'}{w_1}\right) g_1 = \frac{Z_0 g_1}{w_c} = \frac{Z_0 g_5}{w_c} = L_5 \tag{5}$$

$$L_3 = \frac{Z_0 g_3}{w_c} \tag{6}$$

Where, $R_0' = 1$ and $w_1' = 1$ are normalized impedance and frequency, $R_0 = Z_0$ is the characteristic impedance and is the w_c the cutoff frequency of the desired filter. Table 1 shows the initial, the converted, and the alternative values for each of the filter elements. Now, the inductors in the compressed circuit are replaced with parallel LC circuits, according to Fig. 10.

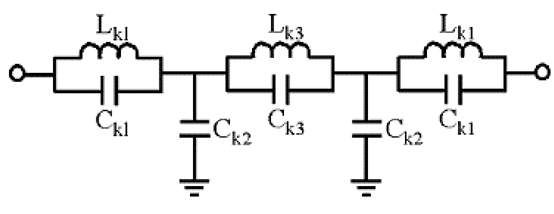

Fig. 10. Modified lowpass sample filter after replacement of each inductor with the LC circuit.

Using (1), (3), and (5), Eq. 7 is obtained to calculate the values of C_{ki} and L_{ki}.

$$\frac{1}{\omega_c L_i} = -\left(\omega_c C_{ki} - \frac{1}{\omega_c L_{ki}}\right) \tag{7}$$

The cutoff frequency of the filter is also obtained by placing the (5) in (7).

$$\omega_c = -\frac{L_{ki}\omega_0^2}{2g_1Z_0} + \sqrt{\frac{\omega_0^4}{4}\left(\frac{L_{ki}}{g_1Z_0}\right)^2 + \omega_0^2} \qquad (8)$$

As mentioned earlier, for the realization of a lowpass filter by defected ground structures, each of the parallel LC components in the converted compressed circuit must be replaced with a cell of the defected ground structure with appropriate dimensions. For this purpose, several butterfly-shaped defected ground structures with different dimensions have been analyzed.

Fig. 11 shows a diagram in which the values of the inductor and the capacitor of the equivalent circuit of the butterfly-shaped DGS are drawn according to the dimensions of the structure (a = b). As can be seen, the changes in capacitor versus changes in the dimensions of the proposed DGS are small and insignificant. Therefore, to simplify and obtain the L_k and C_k values, all C_k can be considered constant and calculate L_k using (7).

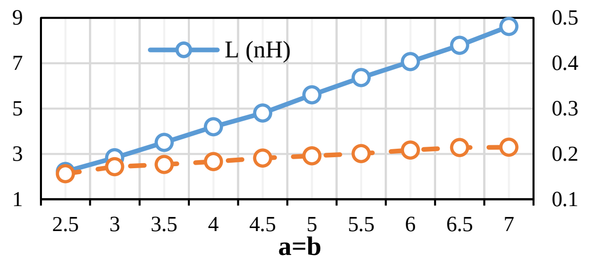

Fig. 11. Values of inductors and capacitors for different dimensions of the proposed structure.

In the design of the mentioned filter, all C_k is considered constant and equal to 0.1883pF, and the values of L_k are determined using (7). The values of the inductors obtained are listed in Table 1.

To design the circuit of the microstrip filter, first, the approximate dimensions of each of the butterfly-shaped defected ground structure cells using Fig. 11 are determined. Then, the precise dimensions of each of the butterfly-shaped defected ground structure cells are specified using the Optimetrics option in HFSS software and performing parametric analyzes and optimizing the obtained results.

Table 1. The values of the initial elements of the five-pole Chebyshev lowpass sample filter with a 0.01dB ripple and the values of its alternative elements.

Initial elements	Initial value	Converted elements	Converted value	Alternative elements	Alternative elements values
g_0	1	Z_0 (Ω)	50	-	-
g_1	0.7563	L_1(nH)	2.5433	L_{k1}	2.3063
g_2	1.3049	C_2 (pF)	1.7552	-	-
g_3	1.5773	L_3 (nH)	5.3041	L_{k3}	4.3684
g_4	1.3049	C_4 (pF)	1.7552	-	-
g_5	0.7563	L_5 (nH)	2.5433	L_{k5}	2.3063
g_6	1	Z_0(Ω)	50	-	-

Assuming constant values $c=1mm$ and $g=0.5mm$, as well as $a=b$ for each cell, for the realization L_{k1}-C_{k1} and L_{k3}-C_{k3} components, values of a and b are obtained $a=b=3mm$ and $a=b=4mm$, respectively. To achieve parallel capacitors C_{k2} and C_{k4} in the filter circuit, which also have equal capacity, two pieces of microstrip transmission line with width $w=1.4mm$ and length $l=6.94mm$ have been used. Each of these components is located between two adjacent defected ground structures. The general schematic of this filter can be seen in Fig. 12. Fig. 13 shows the scattering parameters of the designed filter. As can be seen, this filter has a 3 dB cutoff frequency at 3 GHz and a wide stopband bandwidth of about 10GHz.

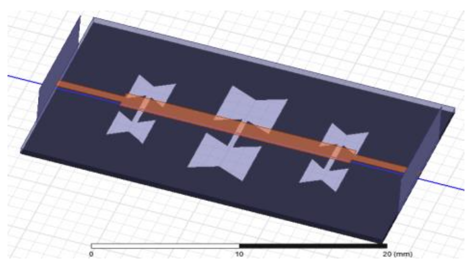

Fig. 12. The general schematic of the designed lowpass filter using the proposed DGS.

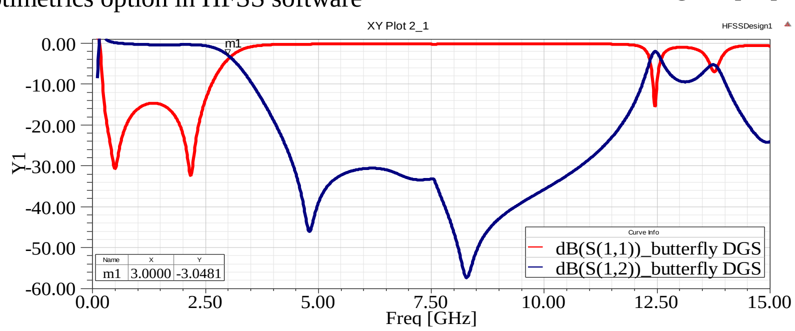

Fig. 13. The scattering parameters of the designed filter using the proposed DGS.

6. COMPARISON OF THE DESIGNED FILTER USING BUTTERFLY-SHAPED DGS

Using the method introduced in [20] with cutoff frequency at 3 GHz, a filter is simulated to investigate and compare the designed filter parameters using the butterfly-shaped DGS. The complementary split-ring resonator (CSRR) defected ground structure is employed to design the filter. For proper comparison, the CER-10 (Taconic) substrate with $\varepsilon r=10$ and thickness $d=0.625mm$ is used in the design and simulation of this filter. The designed filter with CSRR structure is presented in Fig. 14. Also, the frequency characteristic of the filter with the CSRR structure and the filter with the butterfly-shaped structure are shown in Fig. 15. The dimensions of the filter with butterfly-shaped DGS and filter with CSRR DGS are 26×15 mm and 28×14 mm, respectively. As seen in the curves, the cutoff frequency of both filters is 3 GHz. However, the stopband bandwidth with a rejection amplitude of more than -20 dB is 7.64 GHz in the filter with butterfly-shaped DGS and 0.94 GHz in the filter with CSRR DGS. Also, as shown in Fig. 16, the loss in the passband (insertion loss) in the filter with butterfly-shaped DGS is less than the filter with CSRR DGS.

Based on the results, the filter with butterfly-shaped DGS is more efficient than the filter with CSRR DGS in parameters including stopband bandwidth, loss in the passband, and dimensions.

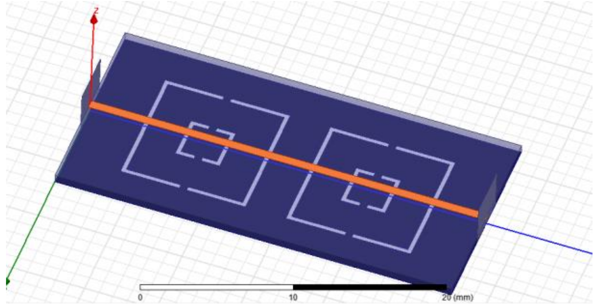

Fig. 14. The general schematic of the designed lowpass filter using the CSRR DGS.

7. COMPARISON OF SIMULATION AND MEASUREMENT RESULTS OF THE DESIGNED FILTER USING BUTTERFLY-SHAPED DGS

The proposed filter is fabricated, and its scattering parameters are measured using the Network Analyzer device to compare and validate the results obtained from the simulation by the HFSS software. Fig. 17, (a) shows the view of both sides of the printed circuit board of the proposed filter. Also, recorded results on the Network Analyzer screen are shown in Fig. 17, (b) and (c).

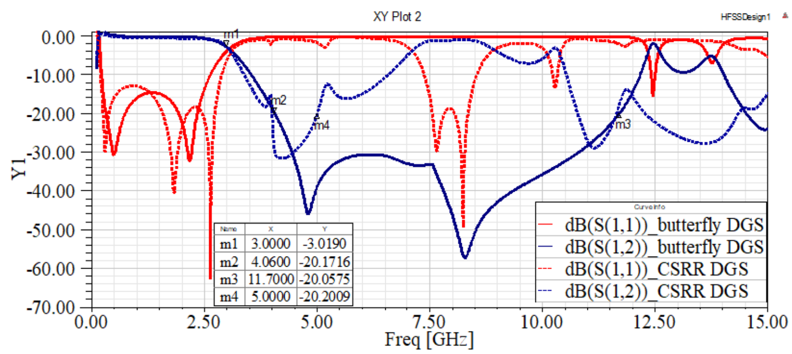

Fig. 15. The scattering parameters of designed filters.

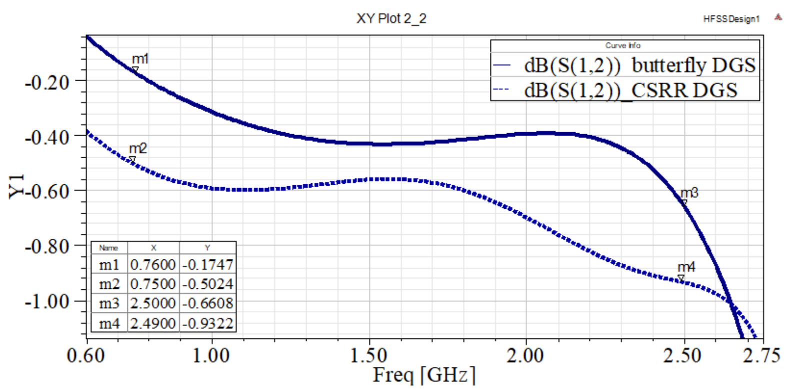

Fig. 16. The insertion loss in designed filters.

(a) (b) (c)

Fig. 17. (a): Front and back views of the fabricated filter, (b) and (c): Measured scattering parameters by Network Analyzer S21 and S11, respectively.

The frequency responses are plotted together in Fig. 18 and Fig. 19 to compare the simulated and measured results. As can be seen, the measured results are close to the simulated results, and the graphs match.

8. CONCLUSION

In this paper, a new defected ground structure called the butterfly-shaped structure is introduced and analyzed. This structure has four degrees of freedom, one degree of more freedom than a conventional rectangular dumbbell-shaped structure. A comparison of the geometrical dimensions of the proposed structure with the dumbbell structure (assuming the same attenuation pole) shows that the area of the proposed structure is reduced by 21.82%.

Also, filter bandwidth increased by 12.94%. In the following, a lowpass filter is designed using a butterfly-shaped defected ground structure and compared with the filter introduced in [20], which uses the CSRR structure. The results reveal that the filter designed with the butterfly-shaped structure is further efficient than the CSRR structure in stopband bandwidth, loss in the passband, and dimension. Finally, after fabricating the designed filter, simulation and measurement results are compared, which shows a proper match.

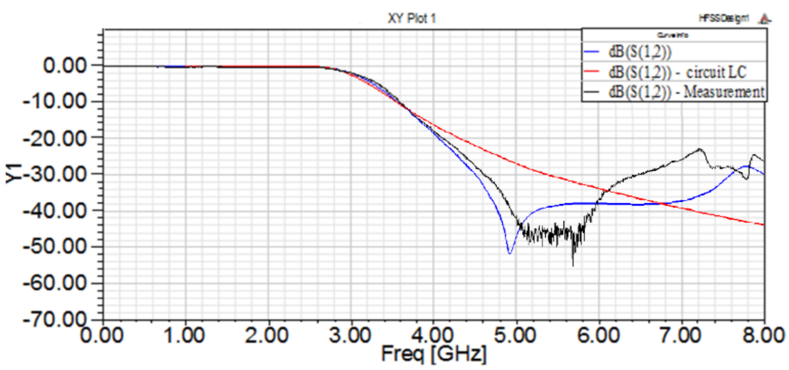

Fig. 18. Comparison of S12 parameters in measurement, simulation, and LC circuit cases.

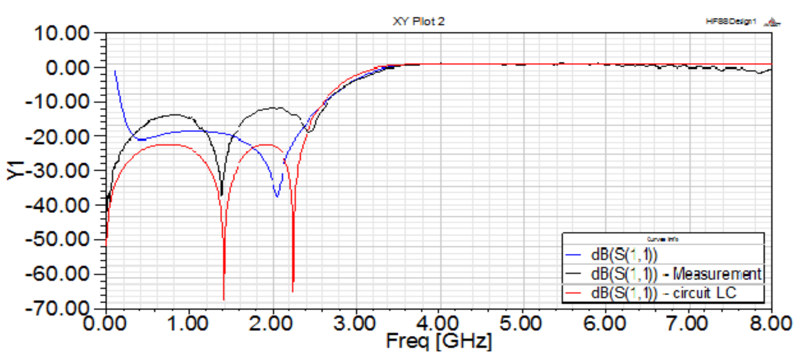

Fig. 19. Comparison of S11 parameters in measurement, simulation, and LC circuit cases.

REFERENCES

[1] K. Wei, J.Y. Li, L. Wang, Z.J Xing, R Xui, "**Mutual Coupling Reduction of Microstrip Antenna Array by Periodic Defected Ground Structures**," *IEEE 5th Asia-Pacific Conference on Antennas and Propagation (APCAP)*, 2016.

[2] A. I. Hammoodi, H. Raad, and M. Milanova, "**Mutual Coupling Reduction between Two Circular Patches Using H-Shape DGS**," *IEEE International Symposium on Antennas and Propagation & USNC/URSI National Radio Science Meeting*, 2018.

[3] Deng, Z., W. Jiang, S. Gong, Y. Xu, and Y. Zhang, "**A new method for broadening bandwidths of circular polarized microstrip antennas by using DGS parasitic split-ring resonators**," *Progress In Electrom*agnetics Research, Vol. 136, 739-751, 2013.

[4] Zhang, J., B. Cui, S. Lin, and X.-W. Sun, "**Sharp-rejection lowpass filter with controllable transmission zero using Complementary Split Ring Resonators (CSRRS)**," *Progress in Electromagnetics Research*, Vol. 69, 219-226, 2007.

[5] Patel, R, A. Desai, and T. Upadhyaya, "**An electrically small antenna using defected ground structure for RFID, GPS and IEEE 802.11 a/b/g/s applications**," *Progress in Electromagnetic Research Letters*, Vol. 75, 75-81, 2018.

[6] Huang, Y., Z. Shao, and L. Liu, "**A substrate integrated waveguide bandpass filter using novel defected ground structure shape**," *Progress in Electromagnetics Research*, Vol. 135, 201-213, 2013.

[7] W. Shanshan, and S. Lizhong, "**Design and simulation of a kind of wide band microwave coupler with defected ground structure**," *IEEE International Conference on Electronic Information and Communication Technology (ICEICT)*, 2016.

[8] He, Z., J. Cai, Z. Shao, X. Li, and Y. Huang, "**A novel power divider integrated with SIW and DGS technology**," *Progress in Electromagnetics Research*, Vol. 139, 289-301, 2013.

[9] A. Khare, S. Kharat, A. Rajapkar, S.M. Rathod, and M. Kulkarni , "**Design of a Compact Wilkinson Power Divider using Four Asymmetric DGS for Harmonic Suppression**," *TEQIP III Sponsored International Conference on Microwave Integrated Circuits, Photonics and Wireless Networks (IMICPW)*, 2019.

[10] R. L. Shao, Y. J. Zhou, L. Yang, and C. Tan, "**Compact meander-slot DGS for MIMO antenna with high isolation**", *2018 International Workshop on Antenna Technology (IWAT)*, pp. 1-3, 2018.

[11] A. Barzgar, and H. Oraizi, "**A low profile band pass DGS filter for harmonic suppression**", *2017 Sensors Networks Smart and Emerging Technologies (SENSET)*, pp. 1-4, 2017.

[12] Chang, C., Y. Qian, and T. Itoh, "**Analysis and applications of uniplanar compact photonic bandgap structures**," *Progress in Electromagnetic Research*, Vol. 41, 211-235, 2003.

[13] D. Ahn, J. S. Park, C. S. Kim, J. Kim, Y. Qian, and T. Itoh, "**A design of the lowpass filter using the novel microstrip defected ground structure**", *IEEE Trans. Microwave Theory Tech.*, vol. 49, pp. 86-93, 2001.

[14] R. Er-rebyiy, J. Zbitou, A. Tajmouati, M. Latrach, A. Errkik, and L. El Abdellaoui, "**A New Design of a Miniature Microstrip Patch Antenna Using Defected Ground Structure DGS**", *Wireless Technologies Embedded and Intelligent Systems (WITS)*, 2017.

[15] S. Verma, D. Rano, and M.S. Hashmi, "**A novel miniaturized band stop filter using fractal type defected ground structure (DSG)**", *IEEE Asia Pacific Microwave Conference (APMC)*, pp. 799-802, 2017.

[16] Wang, C. J. and T. H. Lin, "**A multi-band meandered slotted-ground-plane resonator and its application of lowpass filter**," *Progress in Electromagnetics Research*, Vol. 120, 249-262, 2011.

[17] Chen, J., Z.-B.Weng, Y.-C. Jiao, and F.-S. Zhang, "**Lowpass filter design of Hilbert curve ring defected ground structures**," *Progress in Electromagnetics Research*, Vol. 70, 269-280, 2007.

[18] X. Guan, G. Li, and Z. Ma, "**Optimized Design of a Lowpass Filter Using Defected Ground Structures**," *In proceedings of the Asia-Pacific Microwave Conference*, vol. 1, 2005.

[19] G. L. Matthaei, L. Young, and E. M. T. Jones, Microwave Filters, Impedance-Matching Networks, and Coupling Structures, Artech House Publishers, 1980.

[20] S. Sureshkumar, P. M. Rubesh Anand, A. Prajapati, and K. Sakthidasan Sankaran, "**Low Pass Filter Design with CSRR as Defected Ground Structure**," *IEEE International Conference on Communication and Signal Processing (ICCSP)*, pp. 893-896, 2018.